SOURCE MODEL OF THE 2010 ELAZIG KOVANCILAR EARTHQUAKE (M_w 6.1) FOR BROADBAND GROUND MOTION SIMULATION

Mehmet Baykal* **Supervisor: Hiroe Miyake****
MEE10509

ABSTRACT

On 8 March 2010, an earthquake of M_w=6.1 occurred in Elazig and Kovancilar in Turkey. This event is known as the 2010 Elazig Kovancilar earthquake. It caused massive destruction in the rural areas affected and claimed lives.

We performed the empirical Green's function method to simulate the strong ground motion of this event and the largest aftershock recorded with magnitude M_w=5.5, utilizing strong ground motion data from strong motion and broadband velocity stations. We then converted these records into a uniform sampling frequency to carry out the simulation. Amplitude spectral analysis was used to find an estimation of parameters used in the empirical Green's function method.

The focal mechanism determined by Tan *et al*. (2011) was used for the simulation of the mainshock and the largest aftershock. The best source model was estimated by fitting the synthetic acceleration, velocity and displacement to the observed seismograms.

The obtained size of the estimated strong ground motion generation area was calculated as 2.80 km in length by 2.00 km in width for both the mainshock and the aftershock. The rupture starting point was found to be at northeast and southwest of the estimated strong ground motion area for the mainshock and the largest aftershock, respectively. We determined the scaling parameter for the mainshock as 2 and the stress drop correction factor is 3.5. The determined scaling parameter for the largest aftershock is 2 and the stress drop correction factor is 2.5.

The above analyses suggest that the stress drop correction factor of the strong motion generation area for the mainshock is 1.4 times higher than that for the largest aftershock. The 2010 Elazig Kovancilar earthquake is characterized by shallow depth rupture with high stress drop. This fact is considered to be one of the source effects to generate severe ground motion for the damaging earthquake.

Keywords: Elazig Kovancilar earthquake, empirical Green's function method, strong motion generation area.

1. INTRODUCTION

The 2010 Elazig Kovancilar earthquake (M_w=6.1) at 02:32:30 (GMT) on 8 March, 2010 occurred at the east part of the East Anatolian Fault Zone (EAFZ) in Turkey. The shaking was felt around Elazig, Bingol, Tunceli, Mus, Diyarbakir, and Erzurum cities. The earthquake caused 42 death, 137 injured, 1695 heavily destroyed houses, and 978 partially destroyed houses around Elazig and Bingol cities based on report of Disaster and Emergency Management Presidency of Turkey (DEMP).

*Disaster and Emergency Management Presidency, Turkey.
**Earthquake Research Institute, University of Tokyo, Japan.

Earthquake Department at DEMP reported the magnitude of this earthquake as M_L=5.8 and M_w=6.0, its epicentral coordinates as 38.7665N, 40.0712E which was located in Elazig city in Kovancilar prefecture and with depth of about 5 km. According to the Centroid Moment Tensor solution of the Global GMT Project, this earthquake has a compressional axis on the strike of 228°, dip with 83° and rake angle of -21°. The distribution of the aftershocks indicates that the main fault should be about 25 – 30 km long and 12 – 15 km wide (Figure 1). On the same day, another earthquake occurred at 07:47 (GMT) and the Earthquake Department reported the epicenter coordinates of the second earthquake as 38.7355N , 40.0090E which was located in Elazig – Palu, and its magnitude as M_L=5.6 and the depth of 5 km. According to the Centroid Moment Tensor solution of the Global CMT Project, this earthquake had a compressional axis on the strike of 231°, dip with 78°, and rake angle of -11°.

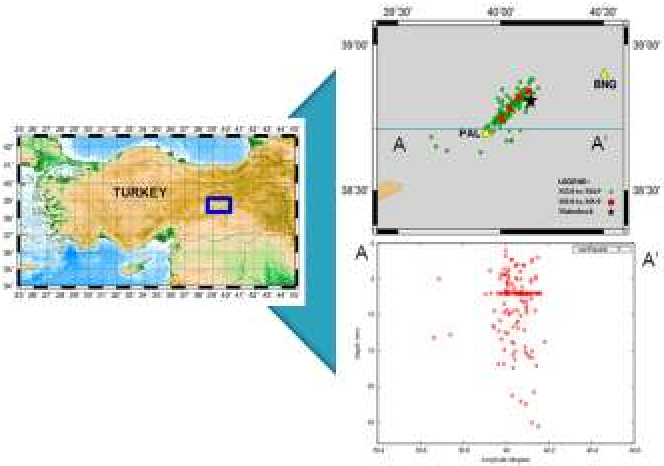

Figure 1. Location of the Kolazig-Kovancilar earthquake is denoted by the black star, the red and green dots are the aftershocks. The yellow triangles are the seismic stations.

According to the recent developments based on waveform inversion of strong ground motion data for estimating the rupture process during large earthquakes, strong ground motion is related to the slip heterogeneity rather than the average slip over the entire rupture area as studied by Irikura and Miyake (2011).The strong ground motions at specific sites near the fault can be estimated by using the empirical Green's function technique. In order to calculate nonlinear dynamic analysis of structures which are needed to design earthquake-resistant buildings, bridges and nuclear power plant, this kind of techniques are used effectively. In addition, most strong motion predictions in earthquake hazard analyses have been made by using empirical attenuation-distance curves for peak ground acceleration (PGA), peak ground velocity (PGV), and response spectra. This information is defined only by magnitude and fault geometry. However, ground motions which caused damage are sometimes characterized by rupture directivity pulses like the 1995 Kobe and the 1999 Izmit earthquakes.

2. DATA

In this study, we used acceleration data that are recorded by National Strong Ground Motion Network (NSGMON) being operated and maintained by the Disaster and Emergency Management Presidency (DEMP), a governmental agency in Turkey. We also used velocity data recorded by Kandilli Observation and Earthquake Research Institute (KOERI) managed by Bogazici University

We selected two events. The first one is the mainshock of the 2010 Elazig Kovancilar Earthquake (M_w=6.1) and the other one is the largest aftershock (M_w=5.5. In addition, we selected another aftershock in order to use as an element earthquake (M_w=4.8) in empirical Green's function method by Tan *et al.* (2011). We used four acceleration data for the mainshock which were retrieved from the stations nearest to the mainshock; these stations are BNG, DYR, ERC, and PAL. The

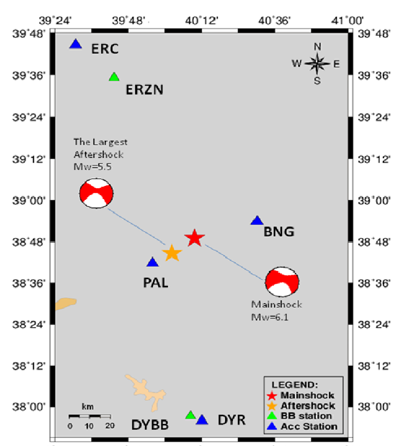

Figure 2. Epicentral location of the mainshock, largest aftershock and location of the stations.

records from the broadband velocity stations were not utilized since these records were clipped and for this reason ERZN and DYBB records for the mainshock cannot be used for the computation of the EGFM. As for the largest aftershock, the data used were from records of the stations BNG, PAL and DYBB. For the element earthquake, records from BNG, PAL and ERC stations were used. Figure 2 shows the station distribution.

.

3. THEORY AND METHODOLOGY

One of the most effective methods for simulating strong ground motion that comes from a large earthquake is to use observed records from small earthquakes occurring around the source area of a large earthquake. Actual geological structure from a source to a site is generally more complex than that assumed in theoretical models. Actual ground motion is complicated as well not only by refraction and reflection due to layer interfaces and ground surface but also by scattering and attenuation due to lateral heterogeneities and inelastic properties in the propagation path. However, main approach for this purpose is to estimate strong ground motion for a large earthquake using the records of small earthquakes which are considered as an empirical Green's function (EGF) by Irikura (1986) and another study by Irikura and Kamae (1994).

The empirical Green's function method takes in on two scaling relations between a large and a small earthquake. They are, a) scaling relations of source parameters, b) scaling relations of source spectra. In the first scaling relations, fault parameters studied by Kanamori and Anderson (1975) are expressed by the Eq(1):

$$\frac{L}{l}=\frac{W}{w}=\frac{T}{\tau}=\left(\frac{M_o}{m_o}\right)^{1/3}=N, \qquad (1)$$

where L and l are fault length, W and w are fault width, T and τ are slip duration time, M_o and m_o are seismic moment, and D and d are fault slip for small and large earthquakes, respectively. The scaling is based on the idea of size independent stress-drop. The second scaling relations are represented by the ω^{-2} source spectra scaling model studied by Aki (1967) and Brune (1970).

Then the spectral relationship between large and small events becomes Eq. (2) and (3)

$$\frac{U_o}{u_o}=\frac{M_o}{m_o}=CN^3, \qquad (2) \qquad\qquad \frac{A_o}{a_o}=CN, \qquad (3)$$

where, U_o, u_o, A_o and a_o are flat levels of displacement spectra and flat level of acceleration spectra for large and small events respectively as shown in Figure 3. The same figure shows the displacement and acceleration source spectra for different sized events predicted by the ω^{-2} model. Where U_o and u_o are flat levels of displacement spectra at low frequencies, f_{cm} and f_{ca} are corner frequencies and A_o and a_o are the flat levels of acceleration spectra at high frequencies between the corner frequency and the cut-off frequency

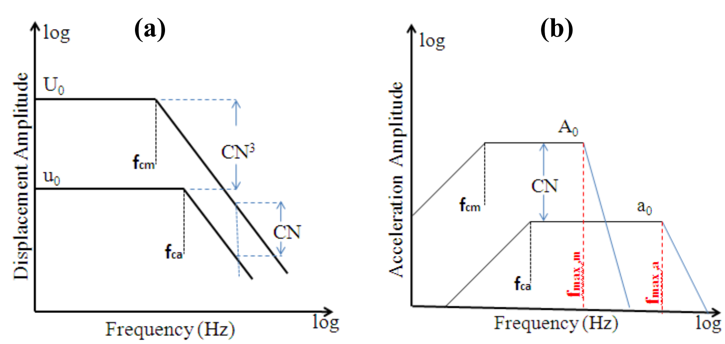

Figure 3. The schematic figures (a) displacement amplitude spectra and (b) acceleration amplitude spectra.

3.1 Formulation for the Simulation

To perform the simulation of the strong ground motion from the large event using the record of a small event as an empirical Green's function, primarily the need to determine the parameters for C and N

which are defined in relations from the Eq. (2) and (3):

$$U(t) = \sum_{i=1}^{N} \sum_{j=1}^{N} \frac{r}{r_{ij}} F(t - t_{ij}) * (C \cdot u(t)), \qquad (4) \qquad t_{ij} = \frac{r_{ij} - r_o}{\beta} + \frac{\xi_{ij}}{V_r}, \qquad (5)$$

$$F(t) = \delta(t - t_{ij}) + \frac{1}{n'(1 - \frac{1}{e})} \sum_{k=1}^{(N-1)n'} [\frac{1}{e^{\frac{(k-1)}{(N-1)n'}}} \delta\{t - t_{ij} - \frac{(k-1)T}{(N-1)n'}\}]. \qquad (6)$$

Observed record from a small event is regarded as an empirical Green's function, and it is summed by following Eq. (4) with time delay according to the scaling law and fault rapture process. The formulation for the EGF method by Irikura (1983; 1986) is based on the deterministic kinematic source model. Ground motion from an earthquake can be expressed as a space-time convolution of slip distribution on the source effect with propagation path effect.

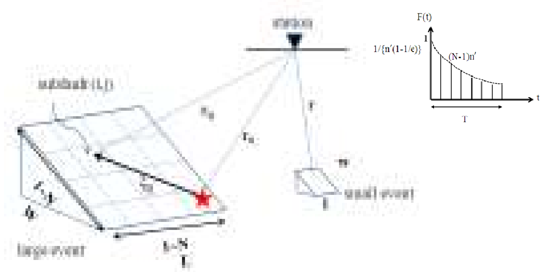

Figure 4. Schematic illustrations of the empirical Green's function method (left of the figure) and filtering function (right of the figure) used in this study.

The source effect of this model is characterized by five parameters in the Eq. (4) and (5): fault length (L and l), fault width (W and w), final offset (r and r_{ij}) (slip), rise time (t and t_{ij}) (slip duration), and rupture velocity (Vr). $U(t)$ is the simulated waveform for the large event, $u(t)$ is the observed waveform waveform for the small event, N and C are the ratios of the fault dimensions and stress drops between the large and small events, respectively, and the * indicates convolution. In the Eq. (6), $F(t)$ is the filtering function (correction function) to adjust the difference in the slip velocity time functions between the large and the small events.

β and V_r are the S-wave velocity near the source area and the rupture velocity on the fault plane, respectively. T is the rise time for the large event, and defined as duration of the filtering function $F(t)$. It corresponds to the duration of slip time function on sub fault from the beginning to the time before the tail starts. n' is an appropriate integer to weaken artificial periodicity of n, and to adjust the interval of the tick to be the sampling rate.

4. RESULTS AND DISCUSSION

For the largest aftershock we determined the value of C equaled to 2.5 and N equaled to 2, thus the possible estimated strong ground motion generation area of the fault was 2 x 2 (Table 1). For this, we

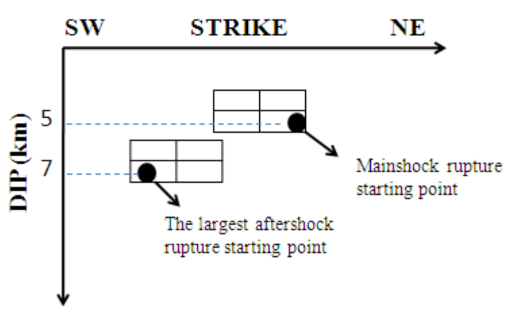

Figure 5. Source parameters of the mainshock and the largest aftershock; the black dots represent the rupture starting points.

Table 1. Calculated scale parameters N and stress drop correction factor C values for the mainshock and the aftershock.

	f_{cm} (Hz)	f_{ce} (Hz)	C	N
Mainshock	0.51	0.73	3.5	2
The largest aftershock	0.53	0.73	2.5	2

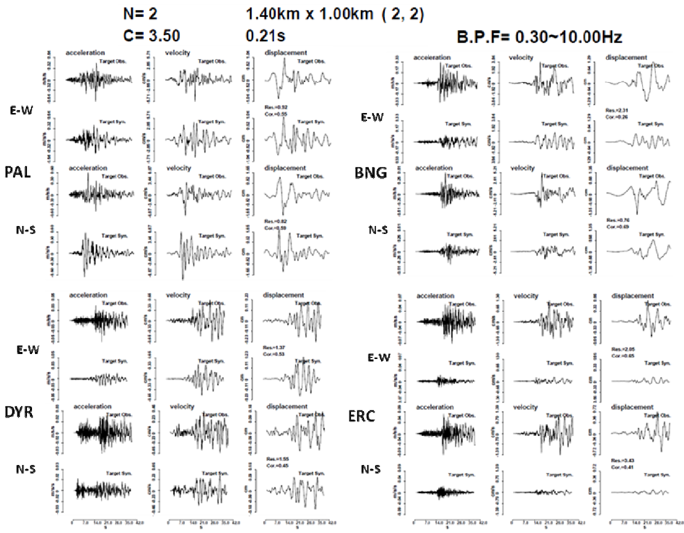

projected 4 cells for the aftershock and the rupture starting point was best located at cell (2, 2) this was proven by the good fit agreement of the observed records and the synthesize motion, which is shown in Figure 5. Figures 6 and 7 compare the observed waveform and synthesized motions.

We compared our results to the scaling relationship of strong motion generation area to seismic moment (Miyake *et al.,* 2003). Our analysis shows that the largest aftershock lies on the same estimated strong ground motion area.

Figure 6. Comparison of observed and synthetic waveforms for the mainshock.

While the mainshock shows it generated a relatively larger seismic moment in comparison to the earthquakes shown in the scaling of the strong motion generation area to seismic moment as shown in Figure 8 (a). Additionally, Figure 8(b) shows the comparison of our results to the scaling relationship of rise time and seismic moment. It suggests that the aftershock occupies the same estimated strong ground motion area. On the other hand, the rise of the strong motion generation area for the mainshock was shorter than the empirical scaling relationship.

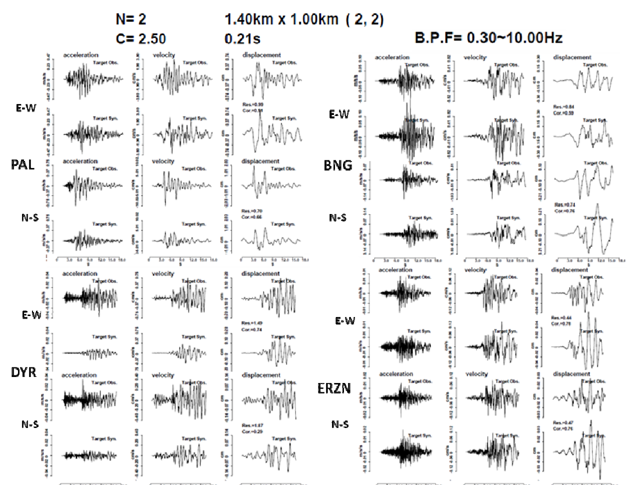

Figure 7. Comparison of observed and synthetic waveforms for the largest aftershock.

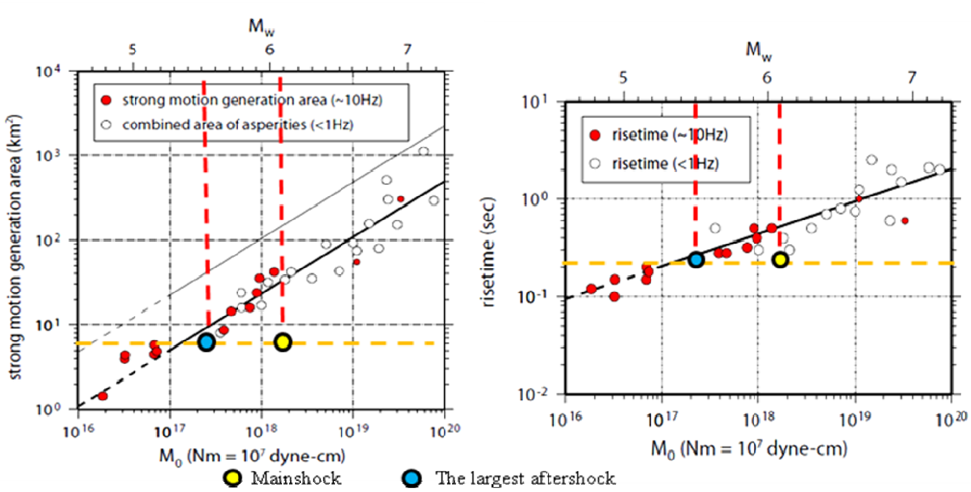

Figure 8. The left graph indicates the scaling between strong motion generation area and seismic moment. The right graph shows the scaling between rise time and seismic moment (Miyake *et al.* 2003).

The mainshock generated seismic moment from the smaller part of the fault plane with a focal depth of 5 km. This might be the reason for the massive destruction caused by the 2010 Elazig Kovancilar earthquake. Another possible reason why we obtained a M6-class earthquake where the absence of any seismic activity recorded in the region.

5. CONCLUSIONS

In this study, we simulated ground motion of the mainshock (M_w =6.1) and that of the largest aftershock (M_w =5.5) for the 2010 Elazig Kovancilar earthquake using the empirical Green's function method. For the simulation, an aftershock with the magnitude M_w =4.8 was selected as an element earthquake. We utilized the data from four acceleration stations and two broadband velocity station records. Using the four strong motion records at the four stations, we calculated the source parameters of the mainshock. The size of strong motion generation area for the mainshock is found to be 2.8 km in length by 2.0 km in width with the rupture starting point at the northeast bottom of the estimated strong ground motion generation area with a depth 5 km and propagated from deep to south-westward with the velocity representing 80% of shear wave velocity. Then we compared the observed records and synthesized motions between acceleration, velocity, and displacement data. The comparison has a good agreement to all the stations used except for the ERC station. We do not have any information about soil condition around the station exactly. However, Erzincan city is located near the Firat river. So, the ERC station might be influenced by some effects of the near surface soil. For this station also, we opted to use ERZN velocity record as an element earthquake. The distance between these two stations is approximately 30 km.

We also simulated the largest aftershock of the Elazig Kovancilar earthquake using three acceleration records and broadband velocity records. The size of the strong motion generation area for the largest aftershock is determined at 2.8 km in length by 2.0 km in width in which the rupture starting point is at southwest bottom part of the estimated strong ground motion generation area towards the northeast with a depth of 7 km. The estimated strong ground motion generation area is located southwest of the mainshock and 4 km away from its epicenter. The above analyses suggest that the stress drop correction factor of the strong motion generation area for the mainshock is 1.4 times higher than that for the largest aftershock. The 2010 Elazig Kovancilar earthquake is characterized by shallow depth rupture with high stress drop. This fact is considered to be one of the source effects to generate severe ground motion for the damaging earthquake.

AKNOWLEDGEMENT

I would like to express my deepest gratitude to my advisor Dr. Toshiaki Yokoi for giving me valuable advises and suggestions.

REFERENCES

Aki, K., 1967, *J. Geophys. Res*., 72, 1217-1231.
Irikura, K., 1986, *Proc. 7th Japan Earthq. Eng. Symp*., 151–156,
Irikura, K. and Kamae, K., 1994, *Annali Di Geofisica*, Vol. XXXVII, N6, 1721-1743.
Irikura, K. and Miyake H., 2011, *Pure and Applied Geophys*., 168, 85-104.
Brune, J. N., 1970, *J. Geophys. Res*., 75, 4997-5009.
Kanamori, H. and Anderson, D., L., 1975, *Bull. Seism. Soc. Am*., 65, 1073-1095.
Miyake, H., Iwata T., and Irikura K., 2003, *Bull. Seism. Soc. Am.*, 93, 2531–2545.
Tan, O., Pabuccu Z., Tapirdamaz M. C., Inan S., Ergintav S., Eyidogan H., Aksoy E., and Kuluozturk F., 2011, *Geophys. Res. Lett.,* 38, L11304, doi: 1029/2011GL047702.